Electrostatic Complexation and Photoinduced Electron Transfer between Zn-Cytochrome *c* and Polyanionic Fullerene Dendrimers

Martin Braun,[a] Stefan Atalick,[b] Dirk M. Guldi,*[b] Harald Lanig,[c] Michael Brettreich,[a] Stephan Burghardt,[a] Maria Hatzimarinaki,[a] Elena Ravanelli,[a] Maurizio Prato,[d] Rudi van Eldik,[e] and Andreas Hirsch*[a]

Abstract: Two dendritic fullerene (DF) monoadducts, **2** and **3**, which can carry up to 9 and 18 negative charges, respectively, were examined with respect to electrostatic complexation with Cytochrome *c* (Cyt*c*). To facilitate comprehensive photophysical investigations, the zinc analogue of Cyt*c* (ZnCyt*c*) was prepared according to a novel, modified procedure. The association of ZnCyt*c* and DF, and consequential photoinduced electron transfer within ZnCyt*c*-DF from the photoexcited protein to the fullerene, was proven by fluorescence spectroscopy and transient absorption spectroscopy. These findings were also supported by circular dichroism as well as by extensive molecular dynamics (MD) simulations.

Keywords: charge separation · dendrimers · fullerenes · metalloproteins

Introduction

Mitochondrial cytochrome *c* (Cyt*c*) is a polycationic redox protein that serves as a mediator for electron-transfer processes in biological systems. We recently discovered that partially deprotonated and therefore negatively charged monolayers of amphifullerene **1**, generated at the air/water interface, show a strong coupling to Cyt*c*, present in the subphase, and lead to the formation of a 3 nm-thick protein layer underneath the amphifullerene layer.[1] The Cyt*c*/fullerene coupling is provided by electrostatic interactions between the two oppositely charged entities. This important finding prompted us to investigate the association and electronic interaction of dendritic fullerenes (DF) **2**[2] and **3** with Cyt*c* in homogeneous solutions. In contrast to the amphiphilic hexakisadduct **1**, water-soluble systems **2** and **3** contain only a single addend covalently attached to the C_{60}

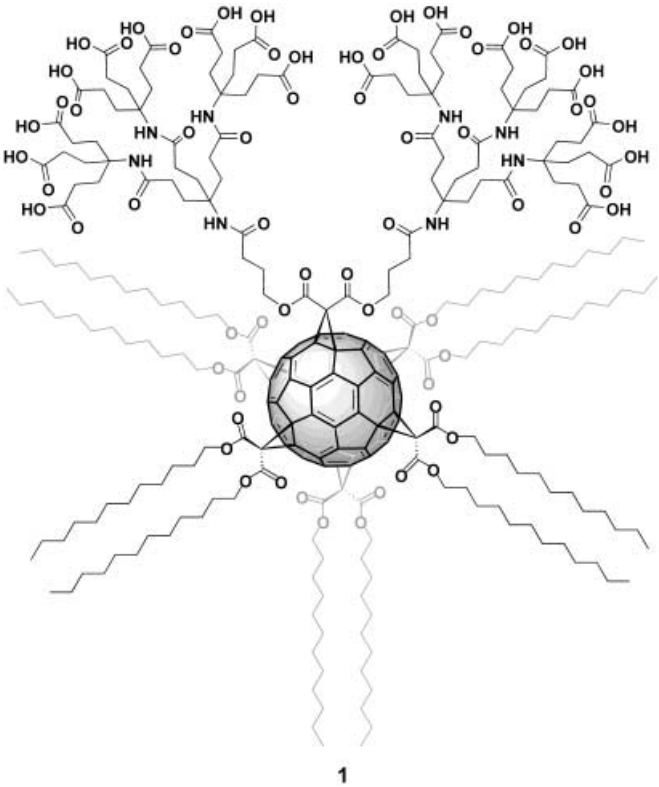

1

[a] Prof. Dr. A. Hirsch, Dipl. Chem. M. Braun, Dr. M. Brettreich, S. Burghardt, Dr. M. Hatzimarinaki, Dipl. Chem. E. Ravanelli
Institut für Organische Chemie
Universität Erlangen-Nürnberg
Henkestrasse 42, 91054 Erlangen (Germany)
Fax: (+49) 9131 8526864
E-mail: hirsch@organik.uni-erlangen.de

[b] Dr. habil. D. M. Guldi, S. Atalick
Radiation Laboratory
University of Notre Dame (USA)

[c] Dr. H. Lanig
Computer-Chemie-Centrum
Universität Erlangen-Nürnberg (Germany)

[d] Prof. Dr. M. Prato
Dipartimento di Scienze Farmaceutiche
Università degli Studi di Trieste (Italy)

[e] Prof. Dr. R. van Eldik
Institut für Anorganische Chemie
Universität Erlangen-Nürnberg (Germany)

 DOI: 10.1002/chem.200204680

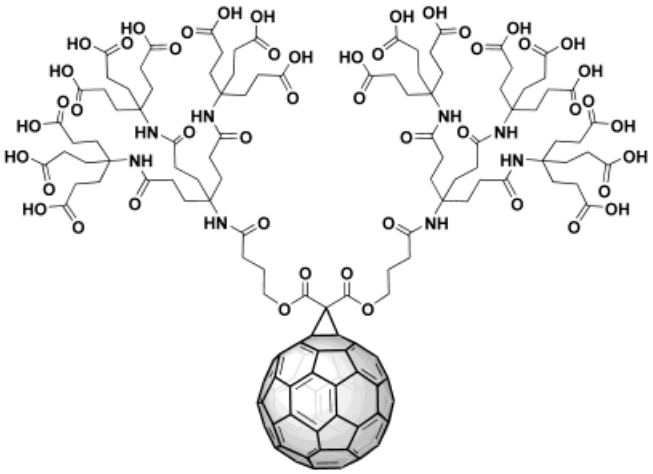

2

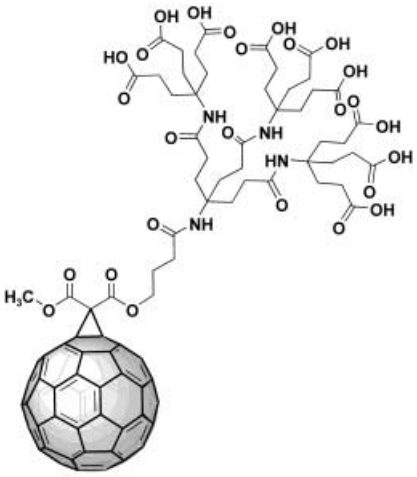

3

core. In monoadducts of C_{60}, the characteristic electron-accepting behavior of the parent system is largely retained, while in hexakisadducts, such as **1**, significant alterations of the fullerene character occur.[3, 4] As a consequence, the fullerene core within **2** and **3** provides a more sensitive probe for the investigation of electrostatic interactions between Cyt*c* and anionic oligoelectrolytes. Hybridization of redox proteins with molecules that modify their electron-transfer properties[5] and conformational behavior,[6, 7] is currently an important topic within bioorganic chemistry.

Results and Discussion

The synthesis of the new water-soluble adduct **3** was performed according to Scheme 1. Starting with the formation of the mono-spacer malonate **8** by a new protective-group strategy and subsequent cyclopropanation of C_{60},[8] the final coupling of the polyamide dendron **11**[9] yielded the dendrofullerene precursor **12**. Cleavage of the *tert*-butyl groups leads to the target compound **3**. The monoadduct **2** was synthesized according to literature procedures.[2] Both dendrofullerene monoadducts **2** and **3** represent oligoelectrolytes, whose number of negative charges (n), which is regulated by the degree of deprotonation of the peripheral carboxylic acid groups, is expected to depend on the pH value of the aqueous solution. Conceptually, the n values can vary between 0 and 18 for **2**, and 0 and 9 for **3**. At a given pH value, the n values of these adducts should be very different and lead to a different interaction with Cyt*c*, which carries eight positive charges at pH 7.[7]

For the analysis of the electrostatic interactions between Cyt*c* and **2** and **3**, respectively, it is mandatory to determine the number of negative charges, n, on the corresponding adducts as a function of pH. We used pH titrations to analyze the range of pK_a values of the carboxylic acid groups and, at the same time, to deduce additional information on the aggregation behavior of **2** and **3**.[10] We discovered that, at the physiological pH of 7.2, adduct **2** carries approximately 16 negative charges, whereas **3** carries about seven negative charges.

By virtue of electrostatic attractions, supramolecular Cyt*c*-DF complexes are assembled in buffered solutions upon simple mixing of Cyt*c* and DF components, namely **2** or **3**. An accurate and widely applied method to investigate such complexes is fluorescence spectroscopy coupled with optical transient absorption spectroscopy. The iron center in the heme group of Cyt*c*, however, exerts a significant deactivation on the excited states of the Cyt*c* porphyrin and, therefore, necessitates replacement, for example, by zinc. In addition, iron ions contain partially filled 3d orbitals and undergo thermal redox reactions. This is in contrast to zinc(II) ions which have a $3d^{10}$ configuration. The inactivity of zinc-substituted hemes in the electronic ground state, as well as its properties in the excited state, renders ZnCyt*c* a very suitable candidate for fluorescence investigations.

ZnCyt*c* is a previously reported derivative of Cyt*c*. It is widely investigated within the scope of conformational fluctuation studies[11] and of complexation studies with porphyrins and other metalloproteins.[12–15] The preparation method of ZnCyt*c* is based on the first method published by Vanderkooi et al.[16, 17] Although several minor modifications of this method concerning buffer, workup, and purification are reported,[11, 14, 18, 19] the crucial step of demetalation of the heme group with anhydrous hydrogen fluoride (AHF), which is difficult to handle, was always performed as described in the original literature.[16, 20] To avoid these handling difficulties, a new method to remove the iron ion was developed that used pyridinium-bound poly(hydrogen fluoride) which is both commercially available and easy to handle.[21, 22] The two-step preparation of ZnCyt*c* starts with the demetalation of commercially available horse-heart ferricytochrome *c* (Fe^{III}-Cyt*c*) with pyridinium poly(hydrogen fluoride). In the second step, zinc was inserted into the heme group of the cytochrome *c*. The thus-obtained ZnCyt*c* was characterized as described in the literature.[17, 18]

In principle, formation of 1:1 and 2:1 complexes may evolve from the association of ZnCyt*c* and **2**. Considering a 2:1 complex for ZnCyt*c*/**2**—see modeling below—we ran parallel assays with ZnCyt*c*/**3**, whose structure precludes a 2:1 stoichiometry.

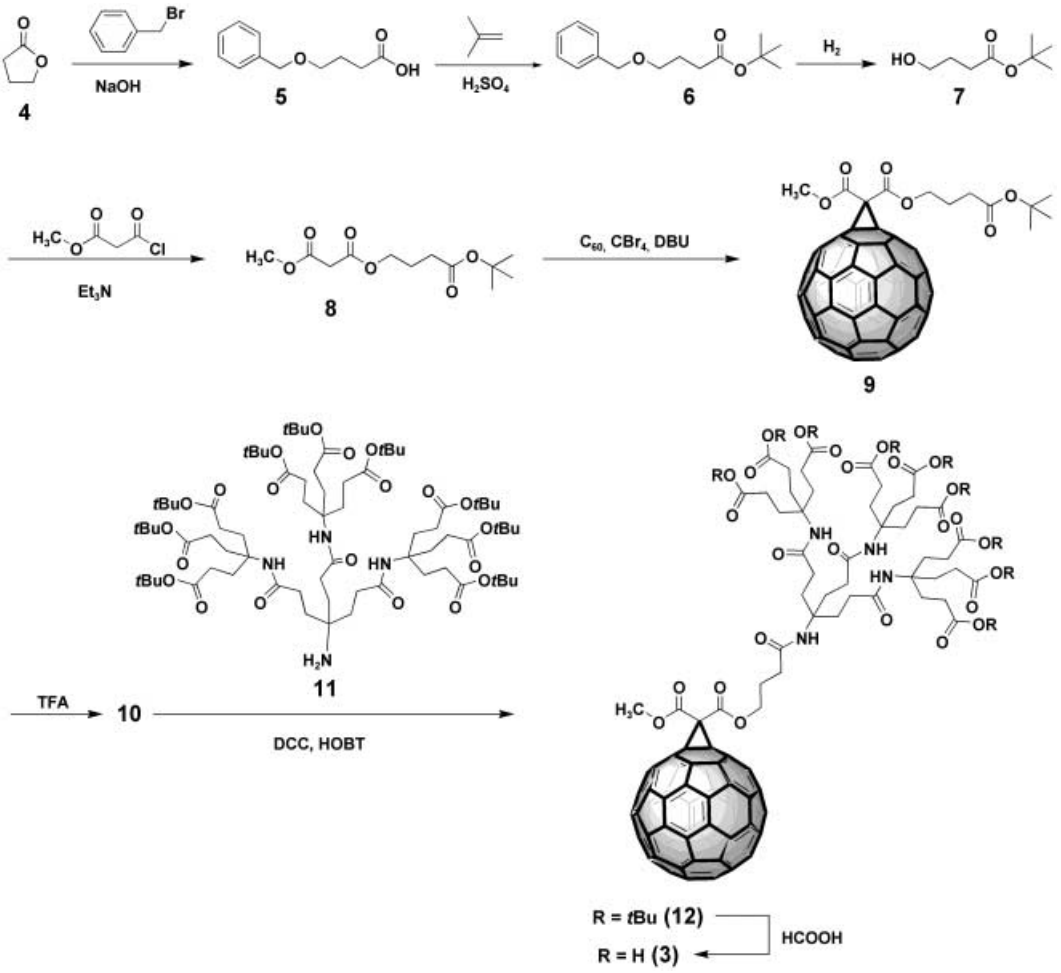

Scheme 1. Synthesis of a new water-soluble dendrofullerene **3**. DBU = 1,8-diazabicyclo[5.4.0]undec-7-ene, DCC = dicyclohexylcarbodiimide, HOBT = 1-hydroxy-1*H*-benzotriazole, TFA = trifluoroacetic acid.

In the associated ensembles (i.e., ZnCyt*c*-DF) the strongly fluorescent ($\Phi \approx 0.04$) and energetically high-lying ($E_{singlet} = 2.1$ eV) photoexcited ZnCyt*c* state, is quenched by an electron-transfer process involving the electron-accepting C_{60} core in DF (vide infra). For example, at pH 7.2 upon titration of a 2.6×10^{-6} M solution of ZnCyt*c* with DF (i.e., either **2** or **3**) in the concentration range $0.38 - 3.5 \times 10^{-5}$ M, the intensity of the ZnCyt*c* emission decreases until a minimum value is reached. Figure 1 documents the ZnCyt*c* emission spectra for a few selected concentrations of **3**. In the minimum region the complexation of ZnCyt*c* is assumed to be complete with an effective ZnCyt*c*-DF concentration of at least 95%.

In Figure 2 the I/I_0 versus concentration relationship is shown for an entire set of concentrations of **3**. The fitting of such titration curves to a previously developed procedure[23] gave values of $1.7(\pm 0.3) \times 10^5\,M^{-1}$ and $3.1(\pm 0.4) \times 10^5\,M^{-1}$ for the stability constants of ZnCyt*c*-**2** and ZnCyt*c*-**3**, respectively, at pH 7.2. These values are in good agreement with previously published stability constants of ZnCyt*c* with fern cupriplastocyanin,[24] plastocyanin,[25] and several free-base porphyrins.[26]

Note that in our fluorescence experiments the effective ZnCyt*c* concentrations are much smaller than those of **2** and **3**, namely [ZnCyt*c*] ≪ [DF]. These conditions are necessary to guarantee a detectable fluorescence quenching, whereas working at [ZnCyt*c*] > [DF], does not lead to any observable changes in the fluorescence spectra. Thus at [ZnCyt*c*] ≪ [**2**],

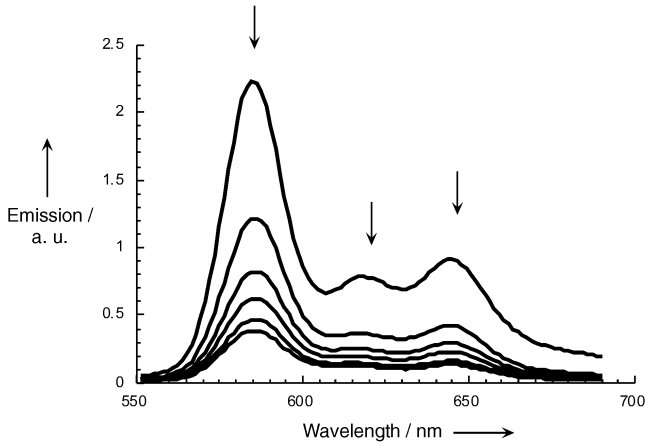

Figure 1. Fluorescence spectra ($\lambda_{exc} = 420$ nm) of ZnCyt*c* (2.6×10^{-6} M) and different concentrations of **3** ($0.38 - 3.5 \times 10^{-5}$ M) in H_2O at room temperature, pH 7.2, 0.05 M Na_2HPO_4. Arrows indicate the decreased fluorescence of ZnCyt*c* with increasing concentration of **3**.

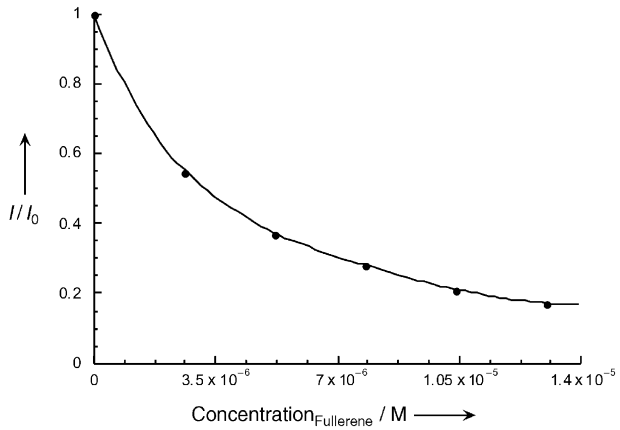

Figure 2. I/I_0 versus [**3**] relationship used to determine the association constant. The fitted curve gives a χ^2 value of 0.00007.

formation of a 2:1 ZnCyt*c*/**2** complex is believed to be precluded. Additional support for this assumption is obtained from the I/I_0 versus [**2**] relationship, for which we only found satisfying fits (i.e., χ^2 at least 0.005) of the experimental data by applying a 1:1 complex stoichiometry.

Prior to the addition of DF, the fluorescence signal of ZnCyt*c* is well fitted by a monoexponential decay, for which a lifetime of 2.98 ns was determined in deoxygenated aqueous solutions at pH 7.2. On addition of **2** or **3**, a double-exponential decay is observed with lifetimes of $\approx$0.26 ns and 2.98 ns, respectively. The two lifetimes are maintained throughout the titration assay, with, however, a relative increase in statistical weight of the short-lived component on increasing the concentration of DF until the plateau region is reached. Addition of acid restores the original fluorescence intensity, concomitant with the disappearance of the short-lived component.

In summary, the decrease in fluorescence intensity in ZnCyt*c* on addition of DF, and the presence of only one short lifetime (0.26 ns), which is invariant throughout the titration assay, suggest a static quenching event inside the well-defined ZnCyt*c*-DF complexes. The restoration of the original fluorescence and the disappearance of the short-lived component upon addition of acid, on the other hand, result from the protonation of the carboxylic groups and the consequent dissociation of ZnCyt*c*-DF into separate fragments.

In the ZnCyt*c*-DF associate, the fluorescent state of ZnCyt*c*, which is a good electron donor ($E_{1/2} = 0.8$ V versus NHE),[27] is quenched by a thermodynamically allowed electron transfer ($-\Delta G_{ET} \approx 0.9$ eV) to the electron-accepting C_{60} moiety of DF (**2**: $E_{1/2} = -0.44$ V versus NHE; **3**: $E_{1/2} = -0.5$ V versus NHE).[28]

The rate constant for the electron-transfer quenching process is obtained from Equation (1), where τ and τ_0 are the short-lived (0.26 ns) and long-lived (2.98 ns) fluorescence components, respectively. The value of k was calculated to be $3.5 \times 10^9\,s^{-1}$.

$$k = \frac{1}{\tau} - \frac{1}{\tau_0} \qquad (1)$$

This estimate is in good agreement with the value derived by Equation (2) ($2.6 \times 10^9\,s^{-1}$), which uses the fluorescence quantum yields Φ recorded for ZnCyt*c* and ZnCyt*c*-**3**.

$$k = \frac{[\Phi(\text{ZnCyt}c) - \Phi(\text{ZnCyt}c\text{-}C_{60})]}{[\tau(\text{ZnCyt}c) \times \Phi(\text{ZnCyt}c\text{-}C_{60})]} \qquad (2)$$

Evidence for an electron-transfer scenario ($-\Delta G_{ET} \approx$ 0.9 eV), opposing to a less exothermic transduction of singlet excited-state energy ($-\Delta G_{EnergyT} = 0.34$ eV), was obtained from transient absorption measurements with ZnCyt*c* and ZnCyt*c*-DF, following 8 ns laser excitation at 532 nm. Differential absorption spectra of ZnCyt*c* in an oxygen-free aqueous solution reveal the growth of a near-infrared absorption centered around 880 nm. Generally, a distinct near-infrared absorption peak in this region is seen in the triplet–triplet absorption spectra of tetraphenylporphyrin-based metalloporphyrins. Thus, we ascribe the transient to the ZnCyt*c* triplet state. In the visible region, additional maxima at 575, 610, and 720 nm and minima at 540 and 580 nm corresponding to ground-state bleaching of the zinc porphyrin Q-band transitions, complete the transient characteristics. The ZnCyt*c* triplet transient decays by a first-order process with a lifetime of 80 ± 10 μs, regenerating the singlet ground state.

A different picture emerges for ZnCyt*c*-DF. Immediately following the short laser excitation into the ZnCyt*c*'s Q bands at 532 nm, spectral characteristics were monitored that correspond to the attributes of the one-electron oxidized form of ZnCyt*c* and the one-electron reduced form of the C_{60} moiety of DF. Maxima in the visible (600–700 nm) and the near-infrared (1040 nm, see Figure 3) clearly attest to the successful formation of ZnCyt$c^{\bullet+}$-$C_{60}^{\bullet-}$, for which we determined a lifetime of 1.8 microseconds in deoxygenated aqueous solutions. The only appreciable changes seen upon varying the concentration of **2** or **3** were different yields of the ZnCyt$c^{\bullet+}$-$C_{60}^{\bullet-}$ radical pair.

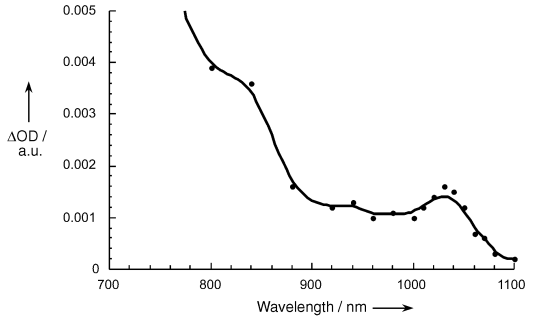

Figure 3. Transient absorption spectrum (NIR part) of ZnCyt*c* (2.6×10^{-6} M) and **3** (3.5×10^{-5} M) in H_2O at pH 7.2, recorded 50 ns after a 8 ns laser pulse ($\lambda_{exc} = 532$ nm), which shows the characteristic $C_{60}^{\bullet-}$ fingerprint with $\lambda_{max} = 1040$ nm.

An elegant means to control the ZnCyt*c*-DF association is to vary the pH and/or the ionic strength of the medium. At pH 6 or 7.2 and by the use of the same C_{60} increments of DF, the fluorescence is, for example, stronger relative to that seen at pH 8.4. This implies less effective interactions between the two redox-active moieties at more acidic pH values. This

assumption is further corroborated by a weaker stability constant (ZnCyt*c*-**3**; pH 6: $1.7(\pm 0.3) \times 10^5\,\text{M}^{-1}$). In contrast, at a more alkaline pH, a higher stability constant (ZnCyt*c*-**3**; pH 8.4: $3.9(\pm 0.5) \times 10^5\,\text{M}^{-1}$) reflects the stronger interactions.

Similarly, ionic strengths of 0.1–0.01M (i.e., Na_2HPO_4-based solutions) effected the ZnCyt*c*–DF association. We noticed differences in K as large as one order of magnitude (ZnCyt*c*-**3**; 0.05M Na_2HPO_4: $3.9(\pm 0.1) \times 10^4\,\text{M}^{-1}$). Considering that HPO_4^{2-}, despite its double charge, possesses a large radius, studies of smaller and single-charged anions were deemed necessary. To explore the function of charge and size, we probed solutions of 0.1M chloride and 0.1M bromide, while keeping the cation (i.e., sodium) constant. The smaller Cl^- is more effective in influencing the ZnCyt*c*–DF association, relative to what we determined for HPO_4^{2-}: a factor of ≈ 2 was found at the same (0.1M) ionic strength. On the other hand, the differences seen between chloride and bromide are insignificant.

As far as the fluorescence lifetime of ZnCyt*c*-**3** is concerned, the presence of the different ions has no impact on the chromophore deactivation.

Contrary to what happens for **2** or **3**, a complementary assay performed with a positively charged *trans*-2 bis-pyrrolidinium[29] salt **13** did not lead to quenching of the ZnCyt*c* fluorescence. The reason for this different behavior relates to

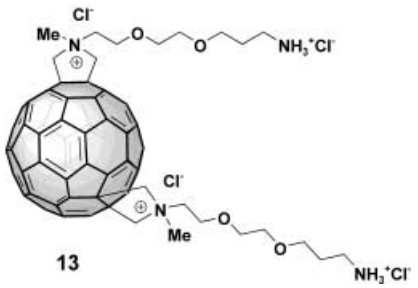

13

the repulsive forces that dominate the interactions between the two fragments. On the nanosecond scale, evidence for the longer-lived triplet excited state is gathered, which then—on the lower microsecond timescale—starts to decay. The triplet decay depends linearly on the bis-pyrrolidinium salt concentration and infers an intermolecular deactivation of ZnCyt*c*. For the reaction of photoexcited ZnCyt*c* with **13**, an intermolecular electron-transfer rate constant of $\approx 10^8\,\text{M}^{-1}\,\text{s}^{-1}$ was determined.

To elucidate further details on the structure of the Cyt*c*-**2** complexes, circular dichroism (CD) spectra and molecular dynamics (MD) simulations were carried out. CD spectroscopy demonstrated that Fe was successfully replaced by Zn since a spectrum (Figure 4) identical to that reported in the literature was obtained.[18] The complexation of ZnCyt*c* with **2** itself is demonstrated by the difference in the CD spectra of parent ZnCyt*c* and ZnCyt*c*-**2** (Figure 4) which is comparable to the changes in the CD spectra observed by the complexation of free base uroporphyrin and tetrakis(4-carboxyphenyl)porphyrin with cytochrome *c*.[26] No indication for significant changes of the protein conformation, either by the

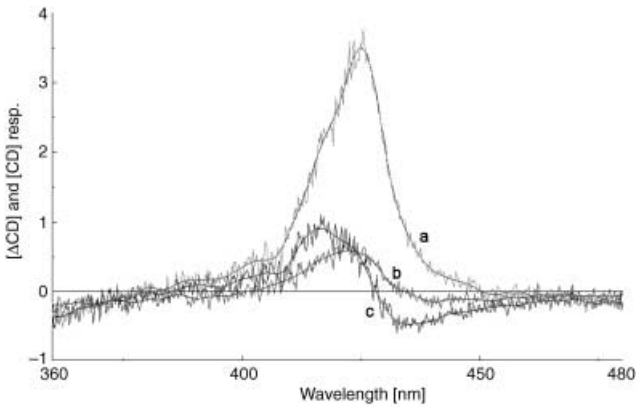

Figure 4. a) Circular dichroism spectra of ZnCyt*c*, b) difference spectra of ZnCyt*c*-**2** hybrids (complexed minus uncomplexed) with 3.6-fold excess of **2**, and c) 13-fold excess.

variation of the preparation method of ZnCyt*c* or by the complexation with **2** was found, since the protein-dominated region of the CD spectra at 200 to 260 nm is not affected.[18] Previous NMR spectroscopic studies also support the fact that the replacement of iron by zinc in Cyt*c* does not cause perturbation of the protein conformation.[30]

By interaction of Cyt*c* with **2**, different complex structures are possible. The distinct 1:1 and 2:1 complexes (Figure 5) were investigated by MD simulations. We used corrected X-ray structure data[31] and a semiempirically optimized

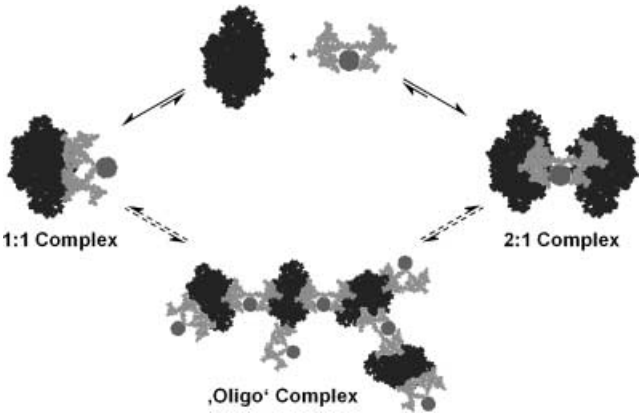

Figure 5. Different possible structures of Cyt*c*-**2** hybrids.

model of **2**. The cytochrome molecule carries a net charge of 8 at pH 7. For the fullerene, almost complete deprotonation of the carboxylic end groups of the dendrimer is assumed on the basis of the titration experiments, which leads to a highly negative net surface charge (Figure 6a). Both molecules were separately preoptimized by a subsequent geometrical force-field optimization and MD simulation over a period of 510 ps. The conformation of the protein remains the same during preoptimization, whereas the charges on the dendrimer sidechains of the fullerene cause a strong electrostatic repulsion and lead to widely extended dendrimer branches. First, we determined whether there is a energetically favored complexation site found for protein–protein complexes at the heme edge region,[32] or if the strong electrostatic attraction

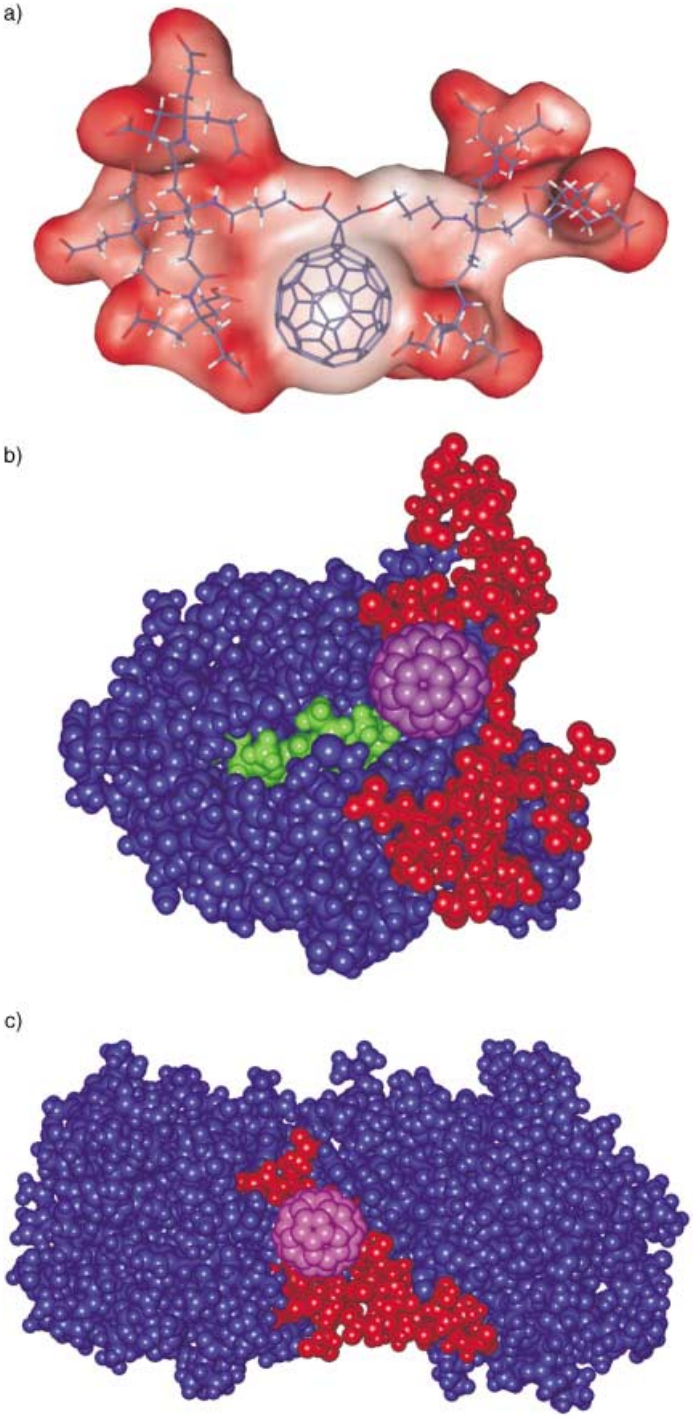

Figure 6. a) Optimized structure (PM3) of $\mathbf{2}^{16-}$ in the gas phase, translucent surface net charge (red). b) Result of the MD simulation of the hybrid Cyt*c*-***2*** with the dendrofullerene **2** directed towards the preferred site for the protein–protein complexes.[25] The fullerene, dendrimer, and heme moieties are colored purple, red, and green, respectively. The protein backbone is shown in blue. c) Result of the MD simulation of the hybrid Cyt*c*-***2*** (2:1 stoichiometry).

does not allow for a specific site selection. Therefore, we compared the number of salt bridges as well as the total energy of six different complexes after MD simulation (see the Experimental Section). In the starting geometry of these six complexes, **2** was located at six cubic sites at a distance of 30 Å to the protein. The resulting complex of the simulation with **2** directed towards the preferred site for the protein–protein complexes[32] is shown in Figure 6b. The simulations revealed no significant difference between the different complexation sites with respect to the observed binding energy or the number and nature of the formed interactions. In addition to the expected salt bridges between the carboxylate end groups of **2** and the charged lysine residues of Cyt*c*, several other interactions with the protein's sidechain as well as with its backbone were observed (Figure 7). Analogous MD simulations of the formation of the 2:1 complexes (Figure 6c) revealed qualitatively the same strong complexation with an over supply in electrostatic interactions. Interestingly, 1:1 complexes of Cyt*c* and **3** show an even stronger interaction than 1:1 complexes with **2**. The complete spatial adaptation of the single dendritic branch of **3** to the surface of the Cyt*c* seems to be facilitated compared to the two dendritic branches of **2**. The major limitation of these calculations carried out in the gas phase is the irreversible formation of the electrostatic interactions between Cyt*c* and DF. However, the gas phase conditions provide the possibility to evaluate many different interaction patterns of such complexes on a reasonable timescale. More detailed simulations of the complexes in a periodic water box are currently under way.

Conclusion

On account of the pronounced electrostatic interaction between the positively charged ZnCyt*c* and the polyanionic dendrofullerenes (DF) **2** and **3**, stable protein–fullerene hybrids are formed. Both the dendrofullerenes and the protein contain redox-active chromophores that can be used as reporter moieties for the detection of hybridization and subsequent electronic interaction within the complexes. If a large excess of DF is used, fluorescent measurements revealed the 1:1 hybrids ZnCyt*c*-**2** and ZnCyt*c*-**3**. The association constants were determined to be $\approx 10^5\,\mathrm{M}^{-1}$. The hybridization to ZnCyt*c*-**2** and ZnCyt*c*-**3** causes fluorescence quenching of the porphyrine emission within ZnCyt*c*. The reason for the fluorescence quenching is a photoinduced electron transfer between the redox protein and the fullerene chromophore.[33] Our photophysical results prove unequivocally that the connection between ZnCyt*c* and DF (either **2** or **3**) is affected by the pH and by the ionic strength of the medium, which leads to an acute control over the number of protonated/deprotonated carboxylate groups of DF. The hybridization leading to ZnCyt*c*-**2** and ZnCyt*c*-**3** was further investigated by CD spectroscopy and molecular modeling. This new hybridization concept that uses the fullerene chromophore as a reporter unit has a great potential for the investigation of electronic and functional properties of a broad range of charged proteins. Moreover, the discovery of very strong electrostatic interactions between the protein and charged dendrimers can be used for the self-assembly of molecular electronic devices. The investigation of layer-by-layer assemblies of Cyt*c* and the dendrofullerenes **2** and **3** leading to photoconductive nanomaterials are currently underway.

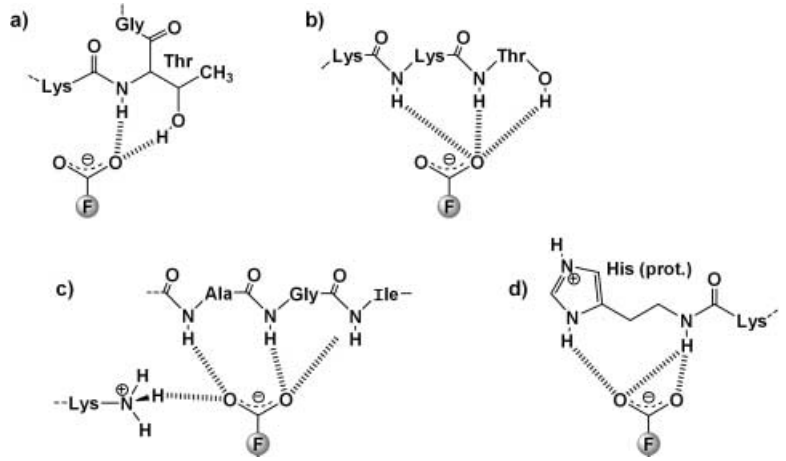

Figure 7. Examples for hydrogen bonding in the Cyt*c*-DF complexes (average length of hydrogen bonds: 1.75 Å).

Experimental Section

General: ^{1}H NMR and ^{13}C NMR: Jeol JNM EX 400 and Jeol JNM GX 400. MS: Varian MAT 311A (EI), Micromass ZabSpec (FAB). UV/VIS: Shimadzu UV 3102 PC. TLC: Merck, silica gel 60 F_{254}. Reagents used were commercially available reagent grade. Solvents were distilled and dried according to standard procedures. Products were isolated where possible by flash column chromatography (silica gel 60, particle size 0.04–0.063 nm, ICN). Compounds **5** and **7** were prepared by modified literature procedures.[34, 35]

Preparation of ZnCyt*c*: This procedure represents a modification of the standard given in the literature and several later alterations.[16, 17] The two-step preparation of ZnCyt*c* includes the demetalation of the commercially available horse-heart FeCyt*c* (*Equus caballus*) and the insertion of zinc into the heme group of Cyt*c*. Horse-heart cytochrome *c* was purchased from Fluka.

Metal-free porphyrin Cytc: FeCyt*c* (103 mg) was dissolved in Py(HF)$_x$ (pyridinium poly(hydrogen fluoride, 6 mL) in a plastic vessel (e.g. PE) inside a strong fumehood at room temperature. The color of the solution changed almost immediately to dark purple. After the mixture had been stirred with a Teflon stirring bar for 10 min at ambient temperature, NH_4OAc buffer (3 mL, 50 mM) was added and the solvent was then removed by a stream of nitrogen. The remaining solid was redissolved in NH_4OAc buffer (6 mL, 50 mM) and purified by gel permeation chromatography with a Sephadex (G-50 "fine") column with the same buffer as the mobile solvent. The main fraction comprising the free-base porphyrin Cyt*c* was eluted first (like normal FeCyt*c*, which has the similar molecular size). After the first sharp fraction, a small amount remained in the tailing of this band; this was discarded. Finally the sample fraction was concentrated to a small volume ($\approx$2 mL) and dialyzed with aid of dialysis tubes against phosphate buffer (pH 7.2) for 1 h. The molecular weight cut-off of the dialysis membranes was 5000. UV/Vis (H_2O) of free-base porphyrin Cyt*c*: λ_{max} (ε) = 274 (36 600), 403 (81 400), 504 (18 700), 539 (16 200), 569 (14 400), 622 nm (12 000).

Insertion of zinc: The metal-free porphyrin Cyt*c* (90 mg) was dissolved in a minimum volume of phosphate buffer and the pH value of the solution was lowered to 2.5 with glacial acetic acid. $ZnCl_2$ or $ZnAc_2$ was added in an approximately 10-fold molar excess, and the mixture was stirred for 30 min in a water bath at 50 °C to complete the reaction. The reconstitution can be monitored by the characteristic bands in the visible absorption spectrum. After the pH was adjusted to 6 with a saturated solution of Na_2HPO_4, ZnCyt*c* was purified by gel filtration. The first and the last portions of the sharp band eluted almost at the front were discarded. Dialysis followed by lyophilization yielded a purple solid, which can be stored at −30 °C in the dark for several months. Since both metal-free porphyrin Cyt*c* and ZnCyt*c* seem to be light-sensitive and less stable then FeCyt*c*, all procedures should be performed under exclusion of light. UV/Vis (H_2O) of ZnCyt*c*: λ_{max} (ε) = 267 (80 300), 356 sh (42 800), 421 (228 000), 547 (17 000), 581 nm (11 700). The total yield of the two steps after lyophilization is 54%.

Preparation of dendrofullerene 3

4-Benzyloxybutyric acid (5): A solution of benzyl bromide (20 mL, 168 mmol) and γ-butyrolactone (3.19 mL, 41.8 mmol) in toluene (75 mL) was treated with freshly crushed 85% KOH (10 g, 178 mmol). The suspension was stirred under reflux for three days, then diluted with Et_2O (40 mL) and H_2O (75 mL). The aqueous layer was washed with Et_2O (2 × 40 mL). The Et_2O/toluene layers were set aside. The aqueous layer was acidified with 3 M H_2SO_4 (40 mL) and the product extracted into CH_2Cl_2. The organic layer was dried over anhydrous $MgSO_4$, filtered, and concentrated under reduced pressure to yield a yellowish oil (2.11 g; 26%). The Et_2O/toluene layer was concentrated to $\approx$80 mL. The solution was treated with a solution of NaOH (4 g) in H_2O (20 mL) and heated to reflux overnight. After hte mixture had been cooled, the aqueous layer was diluted with H_2O (50 mL) and extracted with Et_2O (3 × 20 mL). The aqueous layer was acidified with a slurry of H_2SO_4 (5 mL) in ice (20 mL) and extracted with CH_2Cl_2 (3 × 30 mL). The organic layer was dried over anhydrous $MgSO_4$, and filtered. After removal of the solvent, 5.19 g (64%) of product were obtained. The overall yield was 7.30 g (90%). ^{1}H NMR (400 MHz, $CDCl_3$, RT, TMS): δ = 1.97 (m, 2H; $CH_2CH_2CH_2$), 2.50 (t, ^3J(H,H) = 7.15 Hz, 2H; CH_2COOH), 3.55 (t, ^3J(H,H) = 6.05, 2H; OCH_2), 4.53 (s, 2H; PhCH_2), 7.36 (m, 5H, Ph), 8.90 ppm (br s, 1H; COO*H*); ^{13}C NMR (100.5 MHz, $CDCl_3$, RT, TMS): δ = 24.59 ($CH_2CH_2CH_2$), 30.72 (CH_2COOH), 68.82 (OCH_2), 72.66 (PhCH_2), 127.4, 128.0,128.2, 138.0 (Ph), 179.0 ppm (COOH).

***tert*-Butyl 4-benzyloxybutyrate (6)**: A solution of 4-benzyloxybutyric acid (**5**, 6.96 g, 35.8 mmol) in dry CH_2Cl_2 (30 mL) was treated with condensed isobutene (30 mL at −40 °C) and H_2SO_4 (1 mL). The resultant solution was stirred for three days at room temperature, then neutralized with a solution of K_2CO_3 (5 g) in H_2O (100 mL). The organic layer was washed with K_2CO_3 (saturated solution), citric acid (10 wt% in H_2O), and H_2O. After the mixture was dried over anhydrous $MgSO_4$, filtered, and concentrated, a yellow oil was obtained (7.31 g; 81.4%). ^{1}H NMR (400 MHz, $CDCl_3$, RT, TMS): δ = 1.42 (s, 9H; *t*Bu), 1.89 (m, 2H; $CH_2CH_2CH_2$), 2.32 (t, ^3J(H,H) = 7.15 Hz, 2H; CH_2CO_2tBu), 3.48 (t, ^3J(H,H) = 6.05 Hz, 2H; OCH_2), 4.48 (s, 2H; PhCH_2), 7.31 ppm (m, 5H; Ph); ^{13}C NMR (100.5 MHz, $CDCl_3$, RT, TMS): δ = 25.12 ($CH_2CH_2CH_2$), 27.97 (CH_3), 32.17 (CH_2CO_2tBu), 69.14 (OCH_2), 72.73 (PhCH_2), 79.94 ($C(CH_3)_3$), 127.41, 127.48, 128.23, 138.35 (Ph), 172.7 ppm (CO_2tBu); IR (NaCl): $\tilde{\nu}$ = 3065, 3031, 2976, 2863, 1778, 1730, 1496, 1455, 1392, 1366, 1317, 1254, 1154, 1107, 1029, 959, 908, 847, 736, 698, 612 cm^{-1}.

***tert*-Butyl 4-hydroxybutyrate (7)**: A solution of **6** (7.31 g, 29.2 mmol) in dry ethanol (70 mL) was treated with 10% palladium on carbon (1.22 g) and H_2 at room temperature. After 15 h, the suspension was filtered through Celite and concentrated under reduced pressure to give an oily product in quantitative yield. ^{1}H NMR (400 MHz, $CDCl_3$, RT, TMS): δ = 1.36 (s, 9H; *t*Bu), 1.75 (m, 2H; $CH_2CH_2CH_2$), 2.25 (t, ^3J(H,H) = 7.15 Hz, 2H; CH_2CO_2tBu), 2.79 (br s, 1H; OH), 3.56 ppm (t, ^3J(H,H) = 6.05 Hz, 2H, $HOCH_2$); ^{13}C NMR (100.5 MHz, $CDCl_3$, RT, TMS): δ = 27.75 ($CH_2CH_2CH_2$), 27.92 (CH_3), 32.21 (CH_2CO_2tBu), 61.75 ($HOCH_2$), 80.32 ($C(CH_3)_3$), 173.36 ppm (CO_2tBu); MS (EI): *m*/*z*: 160 [*M*]$^+$, 130, 105, 87, 57, 43; elemental analysis calcd (%) for $C_8H_{16}O_3$ (160.2): C 59.97, H 10.07; found: C 59.90, H 10.21.

Malonate 8: A solution of methyl malonyl chloride (0.67 mL, 6.3 mmol) in dry dichloromethane (5 mL) was added dropwise to a cooled solution (0 °C) of **7** (1.0 g, 6.3 mmol) and triethylamine (0.87 mL, 6.3 mmol) in dry dichloromethane (50 mL) under a nitrogen atmosphere. The mixture was stirred for 2 h at room temperature and then concentrated, and the product was isolated by flash chromatography (silica gel, hexane/ethyl acetate 3:2) and dried in a vacuum. Yield: 1.3 g (5.0 mmol) 80%; ^{1}H NMR (400 MHz, $CDCl_3$, RT, TMS): δ = 1.46 (s, 9H; *t*Bu), 1.96 (m, 2H; CH_2), 2.32 (t, ^3J(H,H) = 7.33 Hz, 2H; CH_2COO), 3.40 (s, 2H; CH_2), 3.77 (s, 3H; OCH_3),

4.20 ppm (t, ^3J(H,H) = 6.41 Hz, 2H; OCH_2); ^{13}C NMR (100.5 MHz, $CDCl_3$, RT, TMS): δ = 23.84 (CH_2), 27.93 (*t*Bu), 31.58 (CH_2COO), 41.13 (CH_2), 52.35 (OCH_3), 64.43 (OCH_2), 80.36 ($C(CH_3)_3$), 166.30 (C=O), 166.80 (C=O), 171.87 (C=O); MS (FAB, NBA): *m*/*z*: 260 $[M]^+$; elemental analysis calcd (%) for $C_{12}H_{20}O_6$ (260.3): C 55.37, H 7.74; found: C 55.10, H 7.73.

Spacer monoadduct 9: DBU (0.2 mL, 1.33 mmol) was added dropwise to a solution of C_{60} (1.0 g, 1.38 mmol), malonate **8** (0.3 g, 1.20 mmol), and tetrabromomethane (0.4 g, 1.20 mmol) in dry toluene (1 L) under a nitrogen atmosphere. The reaction mixture was stirred at room temperature for 20 h, and the progress of the reaction was monitored by TLC. The product was isolated by flash chromatography (silica gel, toluene) and dried in a vacuum. Yield: 270 mg (0.276 mmol) 24%, red brownish solid; ^{1}H NMR (400 MHz, $CDCl_3$, RT, TMS): δ = 1.49 (s, 9H; *t*Bu), 2.16 (m, 2H; CH_2), 2.46 (t, ^3J(H,H) = 7.36 Hz, 2H; CH_2COO), 4.13 (s, 3H; OCH_3), 4.56 ppm (t, ^3J(H,H) = 6.34 Hz, 2H; OCH_2); ^{13}C NMR (100.5 MHz, $CDCl_3$, RT, TMS): δ = 24.11 (CH_2), 28.14 (*t*Bu), 31.69 (CH_2COO), 51.96 ($C_{60}CCOO$), 54.02 (OCH_3), 66.34 (OCH_2), 71.44 (sp^3-C_{60}), 77.20 (sp^3-C_{60}), 80.77 ($C(CH_3)_3$), 138.87, 139.19, 140.96, 140.99, 141.91, 141.93, 142.21, 142.97, 143.02, 143.08, 143.87, 143.89, 144.65, 144.69, 144.91, 145.07, 145.09, 145.16, 145.19, 145.21, 145.24, 145.28, 163.48 (C=O), 164.05 (C=O), 171.82 ppm (C=O); UV/Vis (CH_2Cl_2): λ_{max} (ε) = 257 (107000), 325 (33500), 425 (2300), 476 nm (1500); MS (FAB, NBA): *m*/*z*: 978 $[M]^+$. The purity (99%) was determined by HPLC (on Nucleosil MN, 5 μm, toluene).

Deprotected spacer-monoadduct 10: Trifluoroacetic acid (3.0 mL, 39.0 mmol) was added to a solution of monoadduct **9** (270 mg, 0.276 mmol) in dry toluene (30 mL) under a nitrogen atmosphere. The reaction mixture was stirred for 20 h at room temperature, and the progress of the reaction was monitored by TLC. The reaction mixture was concentrated and dried in vacuum to afford the product. Yield: 240 mg (0.260 mmol) 95%, red brownish solid; ^{1}H NMR (400 MHz, $CDCl_2CDCl_2$, RT): δ = 2.19 (m, 2H; CH_2), 2.60 (t, ^3J(H,H) = 7.08 Hz, 2H; CH_2COO), 4.12 (s, 3H; OCH_3), 4.58 ppm (t, ^3J(H,H) = 6.12 Hz, 2H; OCH_2); ^{13}C NMR (100.5 MHz, $CDCl_2CDCl_2$, RT): δ = 23.59 (CH_2), 29.85 (CH_2COOH), 51.67 ($C_{60}CCOO$), 54.15 (OCH_3), 65.97 (OCH_2), 71.13 (sp^3-C_{60}), 74.29 (sp^3-C_{60}), 138.32, 138.84, 140.50, 140.56, 141.45, 141.74, 142.51, 142.59, 142.65, 143.41, 143.44, 144.12, 144.16, 144.18, 144.20, 144.25 144.47, 144.50, 144.59, 144.69, 144.74, 144.76, 144.82, 163.07 (C=O), 163.62 (C=O), 176.27 ppm(C=O); UV/Vis(CH_2Cl_2): λ_{max} (ε) = 257 (93000), 325 (29000), 425 (2100), 475 nm (1700); MS (FAB, NBA): *m*/*z*: 922 $[M]^+$.

Protected dendrofullerene precursor 12: A solution of dicyclohexylcarbodiimide (0.56 g, 0.270 mmol) and 1-hydroxybenzotriazole hydrate (0.36 mg, 0.270 mmol) was added successively to a cooled solution (0 °C) of monoadduct **10** (240 mg, 0.260 mmol) and dendron H_2N-G2 **11** (0.39 g, 0.270 mmol) in dry THF (25 mL) under a nitrogen atmosphere. The reaction mixture was stirred for 20 h at room temperature, and the progress of the reaction was monitored by TLC. After the mixture was concentrated, the product was isolated by flash chromatography (silica gel, toluene/ethyl acetate 1:1), and dried in a vacuum. Yield: 250 mg (0.107 mmol) 41%, red brownish solid; ^{1}H NMR (400 MHz, $CDCl_3$, RT, TMS): δ = 1.44 (s, 81H; *t*Bu), 1.98 (m, 24H; $C(CH_2\text{-})_3$ + $[C(CH_2\text{-})_3]_3$), 2.03 (m, 2H; CH_2), 2.19 (m, 24H; $CH_2COOtBu$ + CH_2CON), 2.36 (m, 2H; CH_2CO), 4.15 (s, 3H; OCH_3), 4.58 (t, ^3J(H,H) = 6.32 Hz, 2H; OCH_2), 6.22 (s, 3H; NH), 7.68 ppm (s, 1H; NH); ^{13}C NMR (100.5 MHz, $CDCl_3$, RT, TMS): δ = 24.35 (CH_2), 28.06 (*t*Bu), 29.76 (CH_2CON), 29.82 (CH_2COO), 31.58 ($[C(CH_2\text{-})_3]_3$), 31.68 ($C(CH_2\text{-})_3$), 32.63 (CH_2CON), 52.04 ($C_{60}CCOO$), 54.17 (OCH_3), 57.45 ($[C(CH_2\text{-})_3]_3$), 57.57 ($C(CH_2\text{-})_3$), 66.72 (OCH_2), 71.45 (sp^3-C_{60}), 77.19 (sp^3-C_{60}), 80.57 ($C(CH_3)_3$), 139.17, 140.89, 140.96, 141.89, 142.17, 142.18, 142.95, 142.98, 143.02, 143.84, 143.87, 144.58, 144.63, 144.65, 144.67, 144.86, 145.10, 145.15, 145.18, 145.25, 145.27, 163.65 (C=O), 164.13 (C=O), 171.61 (C=O), 172.66 ($-CH_2[COO)_3]_3$), 172.89 ppm($-CH_2(CON)_3$); UV/Vis (CH_2Cl_2): λ_{max} (ε) = 257 (106500), 323 (36500), 425 (4400), 469 nm (3900); MS (FAB, NBA): *m*/*z*: 2345 $[M]^+$, 2367 $[M+Na]^+$. The purity (99%) was determined by HPLC (on Nucleosil MN, 5 μm, toluene/ethyl acetate 3:2).

Dendrofullerene 3: A solution of dendrofullerene **12** (250 mg, 0.107 mmol) in formic acid was stirred for 20 h at room temperature and the progress of the reaction was monitored by TLC. The mixture was concentrated and dried in vacuum to afford the product. Yield: 190 mg (0.103 mmol) 97%, red brownish solid; ^{1}H NMR (400 MHz, D_2O + K_2CO_3 (pH 7), RT): δ = 1.95 (m, 24H; $C(CH_2\text{-})_3$ + $[C(CH_2\text{-})_3]_3$), 2.16 (m, 24H; CH_2COO + CH_2CON and 2H; CH_2), 2.47 (m, 2H; CH_2CO), 4.16 (s, 3H; OCH_3), 4.60 ppm(m, 2H; OCH_2); ^{13}C NMR (100.5 MHz, D_2O + K_2CO_3 (pH 7), RT): δ = 25.45 (CH_2), 27.26, 27.73, 28.02, 28.125, 29.01 (CH_2 dendron and spacer), 30.52 (CH_2CON), 46.30 ($C_{60}CCOO$), 55.22 (OCH_3), 55.60 ($C(CH_2\text{-})_3$), 58.41 (OCH_2), 66.27 (sp^3-C_{60}), 71.61 (sp^3-C_{60}), 138.37, 139.46 140.26, 140.36, 140.49, 141.05, 141.13, 141.30 142.09, 142.54, 143.30, 143.56, 158.82 (C=O), 159.30 (C=O), 172.55 (C=ONH dendron), 172.96 (C=ONH spacer), 180.31 ppm (*C*OOH); UV/Vis (H_2O, pH 7.2 phosphate buffer): λ_{max} (ε) = 254 (88000), 322 (29000), 424 (2500), 466 nm (1700); MS (FAB, NBA): *m*/*z*: 1840 $[M]^+$. The purity (>98%) was determined by NMR spectroscopy.

Photophysics: Fluorescence lifetimes were measured with a Laser Strobe Fluorescence Lifetime Spectrometer (Photon Technology International) with 337 nm laser pulses from a nitrogen laser fiber-coupled to a lens-based T-formal sample compartment equipped with a stroboscopic detector. Details of the Laser Strobe systems are described on the manufacturer's web site, http://www.pti-nj.com. Emission spectra were recorded with a SLM 8100 Spectrofluorometer. The experiments were performed at room temperature. Each spectrum represents an average of at least five individual scans, and appropriate corrections were applied whenever necessary. Nanosecond to millisecond laser flash photolysis experiments were performed with laser pulses from a Quanta-Ray CDR Nd: YAG system (532 nm, 6 ns pulse width) in a front-face excitation geometry. A Xe lamp was triggered synchronously with the laser. A monochromator (SPEX) in combination with either a Hamamatsu R5108 photomultiplier or a fast InGaAs diode was employed to monitor transient absorption spectra.

Computational methods: To examine the electrostatic charge distribution on the protein surface, the program Grasp[36] was used. All other calculations were performed with the program package HyperChem.[37] The employed X-ray structure (PDB code: 1HRC)[31] was corrected at the iron that coordinates His(18) and Met(80) as well as at the two thioether bonds that attach the heme group to the peptide at Cys(17) and Cys(14). The total charge of the protein was kept at +8.0. The Amber89 force-field parameters implemented in HyperChem were used because of the included parameters for the heme groups. Following geometrical optimization, a MD calculation at 300 K for 510 ps was performed to ensure that the protein conformation remains the same. The 16-fold deprotonated dendrimer-containing fullerene was semiempirically optimized (PM3) and also preoptimized by MD calculation for 510 ps. The MD simulations of the complexes were started at a distance between the protein and fullerene of 30 Å, but at different orientations. After heating for 10 ps (1 fs step size) without force-field cut-offs to allow the molecules to attract each other, and to find the first salt bridge contacts, the complexes were kept at 300 K for another 120 ps with force-field cut-offs. Cooling the system to 0 K in 20 ps (without cut-offs) enabled the determination of minimum energies for different complexation possibilities.

Acknowledgement

This work was supported by the Deutsche Forschungsgemeinschaft (SFB 583 Redoxaktive Metallkomplexe—Reaktivitätssteuerung durch molekulare Architekturen), by the European Union under the 5th Framework Programme, HPRNT 1999–00011 FUNCARS, HPRN - CT 2002–00177 WONDERFULL and HPRN - CT 2002–00171 FAMOUS

[1] a) A. P. Maierhofer, M. Brettreich, S. Burghardt, O. Vostrowsky, A. Hirsch, S. Langridge, T. M. Bayerl, *Langmuir* **2000**, *16*, 8884–8891; M. Brettreich, S. Burghardt, C. Böttcher, T. Bayerl, S. Bayerl, A. Hirsch, *Angew. Chem.* **2000**, *112*, 1915–1918; *Angew. Chem. Int. Ed.* **2000**, *39*, 1845–1848.

[2] M. Brettreich, A. Hirsch, *Tetrahedron Lett.* **1998**, *39*, 2731–2734.

[3] A. Hirsch, *The Chemistry of the Fullerenes*, Thieme, Stuttgart, New York, **1994**.

[4] A. Hirsch, *Top. Curr. Chem.* **1999**, *199*, 1–65.

[5] a) S. S. Isied, G. Worosila, S. J. Artherton, *J. Am . Chem. Soc.* **1982**, *104*, 7659–7661; b) S. S. Isied, *Adv. Chem. Series* **1997**, *253*, 331–347; c) J. V. McArdle, H. B. Gray, C. Creutz, N. Sutin, *J. Am . Chem. Soc.* **1974**, *96*, 5737–5741; d) J. V. McArdle, K. Yocon, H. B. Gray, *J. Am .*

Chem. Soc. **1977**, *12*, 4141–4145; d) M. Meier, R. van Eldik, *Inorg. Chim. Acta* **1994**, *225*, 95–101; f) M. Meier, R. van Eldik, I. J. Chang, G. A. Mines, D. S. Wuttke, J. R. Winkler, H. B. Gray, *J. Am . Chem. Soc.* **1994**, *116*, 1577–1578; g) M. Meier, J. Sun, R. van Eldik, J. F. Wishart, *Inorg. Chem.* **1996**, *35*, 1564–1570; h) M. Meier, R. van Eldik, *Inorg. Chim. Acta* **1996**, *242*, 185–189; i) M. Meier, R. van Eldik, *Chem. Eur. J.* **1997**, *3*, 39–46

[6] R. K. Jain, A. D. Hamilton, *Org. Lett.* **2000**, *2*, 1721–1723.

[7] R. K. Jain, A. D. Hamilton, *Angew. Chem.* **2002**, *114*, 663–665; *Angew. Chem. Int. Ed.* **2002**, *41*, 641–643.

[8] X. Camps, A. Hirsch, *J. Chem. Soc. Perkin Trans. 1* **1997**, *11*, 1595–1596.

[9] M. Brettreich, A. Hirsch, *Synlett* **1998**, *12*, 1396–1398.

[10] Detailed results of the titration experiments will be published elsewhere.

[11] Y. Shibata, H. Takahashi, R. Kaneko, A. Kurita, and T. Kushida, *Biochemistry* **1999**, *38*, 1802–1810.

[12] J. M. Vanderkooi, P. Glatz, J. Casadei, G. V. Woodrow, III, *Eur. J. Biochem.* **1980**, *110*, 189–196.

[13] H. Koloczek, T. Horie, T. Yonetani, H. Anni, G. Maniara, J. M. Vanderkooi, *Biochemistry* **1987**, *26*, 3142–3148.

[14] K. T. Conklin, G. McLendon, *J. Am. Chem. Soc.* **1988**, *110*, 3345–3350.

[15] M. M. Crnogorac, G. M. Ullmann, N. M. Kostic, *J. Am. Chem. Soc.* **2001**, *123*, 10789–10798.

[16] J. M. Vanderkooi, M. Erecinska, *Eur. J. Biochem.* **1975**, *60*, 199–207.

[17] J. M. Vanderkooi, F. Adar, M. Erecinska, *Eur. J. Biochem.* **1976**, *64*, 381–387.

[18] S. Ye, C. Shen, T. M. Cotton, N. M. Kostic, *J. Inorg. Biochem.* **1997**, *65*, 219–226.

[19] H. Elias, M. H. Chou, J. R. Winkler, *J. Am. Chem. Soc.* **1988**, *110*, 429–434.

[20] T. Flatmark, A. B. Robinson, in *Structure and Function of Cytochromes* (Ed.: K. Okunuki), University Park Press, Baltimore, Maryland, 318, **1968**.

[21] C. G. Bergstrom, R. T. Nicholson, R. M. Dodson, *J. Org. Chem.* **1963**, *28*, 2633–2640.

[22] G. A. Olah, J. T. Welch, Y. D. Vankar, M. Nojima, I. Kerekes, J. A. Olah, *J. Org. Chem.* **1979**, *44*, 3872–3881.

[23] L. Flamigni, M. B. Johnston, *New. J. Chem.* **2001**, *25*, 1368–1370.

[24] E. V. Pletneva, D. B. Fulton, T. Kohzuma, N. M. Kostic, *J. Am. Chem. Soc.* **2000**, *122*, 1034–1046.

[25] J. S. Zhou, N. M. Kostic, *J. Am. Chem. Soc.* **1991**, *113*, 6067–6073.

[26] R. W. Larsen, D. H. Omdal, R. Jasuja, S. L. Niu, D. M. Jameson, *J. Phys. Chem. B* **1997**, *101*, 8012–8020.

[27] M. C. Crnogorac, N. M. Kositc, *Inorg. Chem.* **2000**, *39*, 5028–5035.

[28] Unpublished data.

[29] S. Foley, S. Bosi, C. Larroque, M. Prato, J.-M. Janot, P. Seta, *Chem. Phys. Lett.* **2001**, *350*, 198–205.

[30] H. Anni, J. M. Vanderkooi, L. Mayne, *Biochemistry* **1995**, *34*, 5744–5753.

[31] G. W. Bushnell, G. V. Louie, G. D. Brayer, *J. Mol. Biol.* **1990**, *214*, 585–595.

[32] H. Pelletier, J. Kraut, *Science* **1992**, *258*, 1748–1755.

[33] Recently, photoinduced electron transfer was found to occur also between a negatively charged conjugated polymer and Cyt*c*; C. Fan, K. W. Plaxco, A. J. Heeger, *J. Am. Chem. Soc.* **2002**, *124*, 5642–5643.

[34] B. G. Szczepankiewicz, C. H. Heathcook, *Tetrahedron* **1997**, *53*, 8853–8870.

[35] H. R. Kricheldorf, J. Kaschig, *Liebigs Ann. Chem.* **1976**, 882–991.

[36] A. Nicholls, K. A. Sharp, B. Honig, *Proteins: Struct. Funct. Genet.* **1991**, *11*, 281–296.

[37] HyperChem 6.03 and 7.0 evaluation release HyperCube, Inc., Gainesville, FL, USA.

Received: December 18, 2002
Revised: March 26, 2003 [F4680]

